Journal of Mathematical Techniques in Modeling
Vol. 1, Issue. 2, 2024
https://doi.org/10.56868/jmtm.v1i2.44

Research Paper https://www.ufpub.com/index.php/jmtm/index

Coherent Manipulation of Distinct Three-Dimensional Localized Shapes of Atoms in Atomic Medium

Najm Uddin[1,*], Attaullah Khan [1,*], Ashfaq Uddin[2], Aisha[2], Sara Gull[2]

1. Department of Physics, University of Malakand, Chakdara 18800, KPK Pakistan

2. Department of Physics Govt Ghazi Umara Khan Degree College Samar Bagh Dir Lower, KPK Pakistan

---

ABSTRACT

This study investigates wall-like, ellipsoidal, and cylindrical structures of atomic localization using an innovative spectrum absorption method including three distinct levels of single atom localization at both the upper and lower sections. The phases, detunings, intensities, and orientations of the applied control fields govern and alter the probability and location of localized atoms. Modified configurations of atom localization are beneficial for Bose-Einstein condensation, atom nanolithography, and laser cooling techniques.

Keywords: Atomic Localization; Density Matrix Formalism; Optical Susceptibility; Bose-Einstein Condensation, Atom Nanolithography

[*]**Corresponding Author**: attaullahphysics@gmail.com
Received: November 05, 2024**; Received in the Revised form:** December 17, 2024; **Accepted:** December 22, 2024
Available online: December 25, 2024

1 Introduction

The precise and reliable assessment of an atom's location within a wavelength range is known as "atom localization". The concept of atomic localization, also known as atomic microscopy, originates from the uncertainty principle as applied through the Heisenberg microscope [1]. The precise position measurements of an atom are measured to (λ/2) of the wavelength, by using Heisenberg microscope [2, 3]. The atom is localized in one-, two-, and three-dimensional spaces, both experimentally and theoretically. After that atom is localized theoretically in one dimension to $(\frac{\lambda}{20})$. Further the atom is localized in two-dimensional space to the accuracy of area $(\frac{\lambda}{10}\ \frac{\lambda}{10})$. Recently atom is also localized in the three-dimensional space of volume $(\frac{\lambda}{10}\ \frac{\lambda}{10}\ \frac{\lambda}{10})$. More accurately atom is localized to $(\frac{\lambda}{1000})$ in one-dimension $(\frac{\lambda}{1000}\ \frac{\lambda}{1000})$ in two-dimension and $(\frac{\lambda}{1000}\ \frac{\lambda}{1000}\ \frac{\lambda}{1000})$ in three-dimension space in the range of one wavelength domain along each x, y and z dimensions. The information of atom localized is extracted from absorption and emission spectra.

Given its significant applications in technology, researchers have extensively studied atom localization using various techniques and mechanisms. Atomic Probe Analysis possesses widespread applications in Bose-Einstein condensation [4], sub-wavelength mapping, microscopy [5], neutral atom capturing and laser cooling [6]. The link between lithography and atom localization were first studied experimentally using standing wave field formalism [4].

Different optical techniques are used for atom localization in one, two, and three dimensions. First, one-dimensional (1D) single-atom localization has been studied, and then two dimensional atom microscopy has been modified. Recently, three-dimensional atom localization was additionally suggested for accurate location measurement [7-10]. Cohen-Tannoudji and his team modified an alternative Heisenberg microscope which works on a single atomic beam and single dimensional standing wave in the experimental setup [11]. Thomas clarified ultra-high precise location measurements for atoms using the modified forms of Heisenberg microscope [12, 13]. Thomas *et al.* [14, 15] actually demonstrated the exact determination of atom location using standing wave optical field.

Numbers of significant and useful works on atom localization have been published on optical techniques and mechanisms [16-21]. Thomas and Zhang [22] discuss useful assessment of these efforts. Other methods for examining the localization of atoms have also been established throughout the past 20 years [23-25]. Further spontaneous emission spectrum is used to explore short wavelength atom localization [26]. Sub wavelength localization has additionally been investigated using atomic coherent effects through the application of electromagnetically generated transparencies [27], dual darkness resonance [28] and coherence concentration trapping [29]. The methods of super-fluorescence [30], dynamically produced coherent [31], dual photon spontaneously released detection [32] and Autler-Townes doublet are also used for atoms localization.

A large number of research articles have been published on two and three atom localization using different mechanisms and techniques in which some of them are mentioned above. But in my knowledge no work is available in the literature to control and modifying topological shapes of atoms by application of coherent driving fields. In this work a four-level atomic system driving by a weak probe field and three control fields is used to investigate topological shapes of atoms localization in a wavelength domain along each axes.

2 Numerical analysis

This section presents the structure and features of a three-level κ-type atomic arrangement, illustrated in Figure 1. The setup consists of two bottom states. |1⟩ and |2⟩ and an excited state |3⟩. A probe field having Rabi frequency of Ω_p and a detuning of Δ_p ties the state together |1⟩ and |3⟩. Similarly, the state is |2⟩ coupled to |3by a field under control through a Rabi frequency of Ω_1 and a detuning of Δ_1. The rate at which states degrade |3⟩ and |1⟩ is denoted as γ_1, and the decay rate between states |3⟩ and |2⟩ is denoted s γ_2.

The Hamiltonian interaction of connection yields as;

$$H_I = -\frac{\hbar}{2}[\Omega_p e^{-i\Delta_p t}|1\rangle\langle 3| + \Omega_1 e^{-i\Delta_1 t}|2\rangle\langle 3| + H.C \tag{1}$$

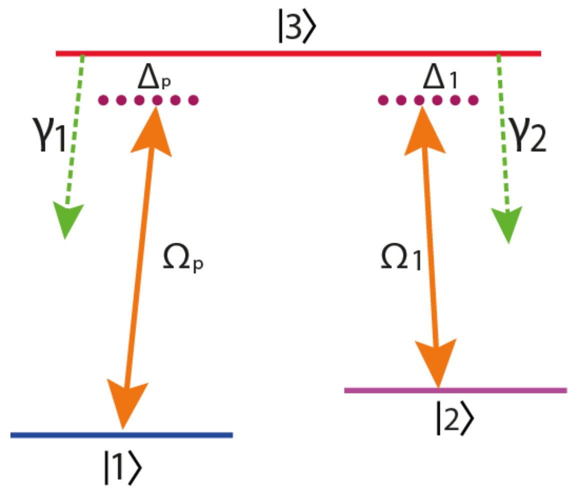

Figure 1. Three-level atomic system

A coherence in electrical susceptibility for optical response is changed using Lindblad's density matrices formula.

$$\dot{\rho} = -\frac{i}{\hbar}[\rho, H_I] - \frac{1}{2}\Sigma\gamma_{ij}\left(\alpha^{\dagger}\alpha\rho + \rho\alpha^{\dagger}\alpha - 2\alpha\rho\alpha^{\dagger}\right), \tag{2}$$

Here, α and α† are the lowering and rising operators respectively, γ_{ij} represent decay rate and H.C. is the Hermiation conjugation factor.

The detuning Δ_p and Δ_1 is given as;

$$\Delta_p = \omega_{13} - \omega_p,\ \Delta_1 = \omega_{23} - \omega_3,$$

The following are the couple rate equations obtained for the probe field of rabi frequency:

$$\dot{\tilde{\rho}}_{13} = \mathrm{M}\tilde{\rho}_{13} + \frac{i}{2}\Omega_p\tilde{\rho}_{33} - \frac{i}{2}\Omega_p\tilde{\rho}_{11} - \frac{i}{2}\Omega_1\tilde{\rho}_{33} \tag{3}$$

$$\dot{\tilde{\rho}}_{12} = \mathrm{N}\tilde{\rho}_{12} + \frac{i}{2}\Omega_p\tilde{\rho}_{32} - \frac{i}{2}\Omega_p\tilde{\rho}_{11} - \frac{i}{2}\,\Omega_1^*\tilde{\rho}_{13} \tag{4}$$

Where M and N are constants.

$$\mathrm{M} = i\Delta_P - \frac{1}{2}\gamma_1 \tag{5}$$

$$\mathrm{N} = i\Delta_P - i\Delta_1 - \frac{1}{2}(\gamma_1 + \gamma_2) \tag{6}$$

Using equation (3) and equation (4), we get

$$\rho_{13} = -\frac{2iM\Omega_p}{4MN+\Omega_1^2} \tag{7}$$

The optical susceptibility is directly linked to the transition element ρ_{13} as is well established for position-dependent optical susceptibility.

$$\chi_e = \frac{2N\sigma_{13}^2\rho_{13}}{\epsilon_0\hbar\Omega p} \tag{8}$$

The Rabi frequency is given as;

$$\Omega_1 = R_1(\mathrm{Sin}[\eta_1 kx] + \mathrm{Sin}[\eta_1 ky + \phi_1 y] + \mathrm{Sin}[\eta_1 kz + \phi_1 z]) \tag{9}$$

3 Result and Discussion

The outcomes of three-dimensional atomic localization within a three-level atomic medium are shown in this section. The imagined element of electrical susceptibility is graphed against the geographic coordinates' kx, ky, and kz to accomplish this. It contains data on the locations and presence of atoms $-\pi <$ kx, ky, kz $< \pi$ and using atomic units variables γ = 1GHz, n = 1, c = 137, $\lambda = \frac{2\pi c}{\omega}$, k = $\frac{2\pi}{\lambda}$ and γ is employed in scaling all other parameters η.

In Figure 2, the specified parameters are used to detect single-atom localization. Δ_1= - 0.3γ, Δ_p= 0.9γ, γ_1=0.02γ, γ_2=0.09γ, Ω_{2a}=1γ, Ω_{20}=6γ, $\phi_{,21,22,23} = \pi$, The observed atom is localized at the top of the first quadrant by applying the applied fields directives $\eta_{1,2,3} = 1$, as shown in Fig 2.a. Through changing the instructions to η_1= -1, $\eta_{2,3}$=1. The localized atom moves to the top of the boxes of second quadrant, as shown in Fig 2.b. Shifting the fields' positions to $\eta_{1,2}$ = -1, η_3 = 1 the localized atom's location changes to the upper third quadrant, as shown in Fig. 2.c. The location of the atom is examined using the field directions in the fourth quadrant of the box $\eta_{1,3}$ = 1, η_2 = -1 as shown in Fig 2.d.

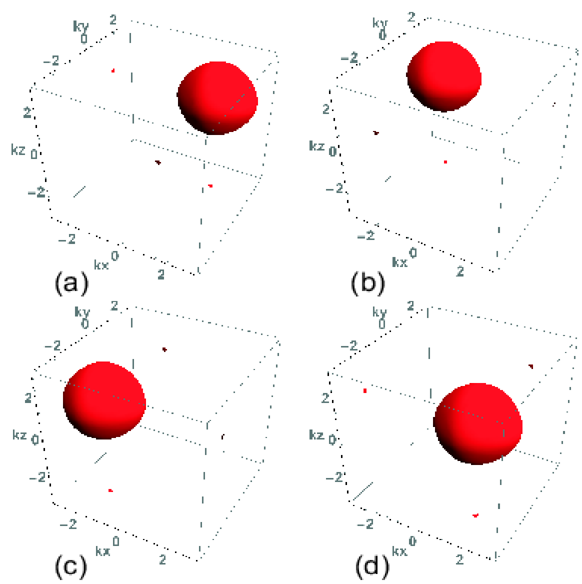

Figure 2: Plots representing the imaginary component of electric susceptibility for kx, ky, and kz, showing atom localization under varying field directions η_1, η_2, η_3 (a) $\eta_{1,2,3}$=1 (b) η_1=−1,$\eta_{2,3}$=1 (c) $\eta_{1,2}$=−1,η_3=1 (d) $\eta_{1,3}$=1,η_2=−1. Parameters: Δ_1=−0.3γ, Δ_p=0.9γ, γ_1=0.02γ, γ_2=0.09γ, Ω_{2a}=1γ, Ω_{20}=6γ, $\phi_{21,22,23}$=π

In Figure 3, Plotting of the imaginary component of electric susceptibility is carried out for k_x, k_y, and k_z locations. Observing a single localized atom requires taking the $\Delta_1 = -0.3\gamma$, $\Delta_p = 0.9\gamma$, $\gamma_1 = 0.02\gamma$, $\gamma_2 = 0.09\gamma$, $\Omega_{2a} = 1\gamma$, $\Omega_{20} = 6\gamma$, $\phi_{21, 22, 23} = \pi$. Using the directions of applied fields, the localized atom investigates at the bottom of the first quadrant $\eta_{1, 2} = -1$, $\eta_3 = -1$ as demonstrated in Fig 3.a. By varying the direction to $\eta_{1, 3} = -1$, $\eta_2 = 1$, at the bottom of the box, in the second quadrant, the localized atom moved, as shown in Fig 3.b. As we shift the directions of the applied fields to $\eta_{1, 2, 3} = -1$, the atom shifts to the lower third quadrant of its location, as shown in Fig 3.c. Applying the directions of the applied fields, the atom's location is seen at the bottom of the box in the fourth quadrant $\eta_1 = 1$, $\eta_{2, 3} = -1$ as shown in Fig 3.d.

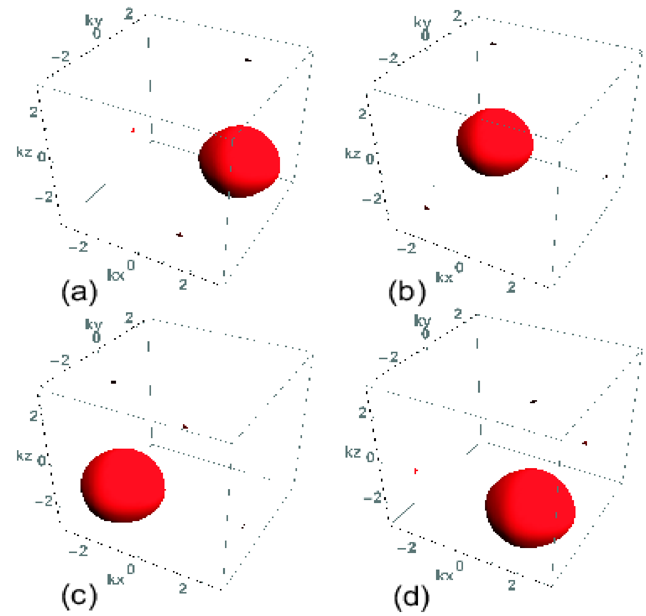

Figure 3: Plotting of the Imaginary component of electric susceptibility for kx, ky and kz, showing atom localization at the box's bottom under field directions: (a) $\eta_{1,2} = -1$, $\eta_3 = -1$ (b) $\eta_{1,3} = -1, \eta_2 = 1$ (c) $\eta_{1,2,3} = -1$ (d) $\eta_1 = 1, \eta_{2,3} = -1$. Parameters: $\Delta_1 = -0.3\gamma$, $\Delta_p = 0.9\gamma$, $\gamma_1 = 0.02\gamma$, $\gamma_2 = 0.09\gamma$, $\Omega_{2a} = 1\gamma$, $\Omega_{20} = 6\gamma$, $\phi_{21, 22, 23} = \pi$

In Figure 4, for the positions kx, ky, and kz, the imaginary component of electric susceptibility is shown. Walk like atoms localization is investigated. Along the diagonal, three wall-like localizations are seen while using the parameters $\Delta_1 = -0.361\gamma$, $\Delta_p = 2\gamma$, $\gamma_{1, 2} = 0.02\gamma$, $\Omega_{2a} = 1\gamma$, $\Omega_{20} = 6\gamma$, $\phi_{21} = \frac{\pi}{3}$, $\phi_{22} = \frac{\pi}{2}$, $\phi_{23} = \frac{2\pi}{2}$, and directions of applied fields $\eta_1 = -0.01$, $\eta_{2,3} = 0$ as demonstrated in Fig 4 . a. By adjusting the parameters $\Delta_1 = -0.3\gamma$, $\Delta_p = 9\gamma$, $\gamma_1 = 0.02\gamma$, $\gamma_2 = 0.09\gamma$, $\Omega_{2a} = 0.01\gamma$, $\Omega_{20} = 6\gamma$, $\phi_{21, 22, 23} = \pi$, & directions of applied fields $\eta_1 = 0.1$, $\eta_{2, 3} = 0.01$ the localization moves to other diagonal as shown in Fig 4 . b. Six wall like localization is examine in other diagonal by distinct variables $\Delta_1 = -0.3\gamma$, $\Delta_p = 0.9\gamma$, $\gamma_1 = 0.02\gamma$, $\gamma_2 = 0.09\gamma$, $\Omega_{2a} = 0.01\gamma$, $\Omega_{20} = 6\gamma$, $\phi_{21, 22, 23} = \pi$, and directions of applied fields $\eta_1 = -1$, $\eta_{2, 3} = -0.01$ as shown in Fig 4.c.

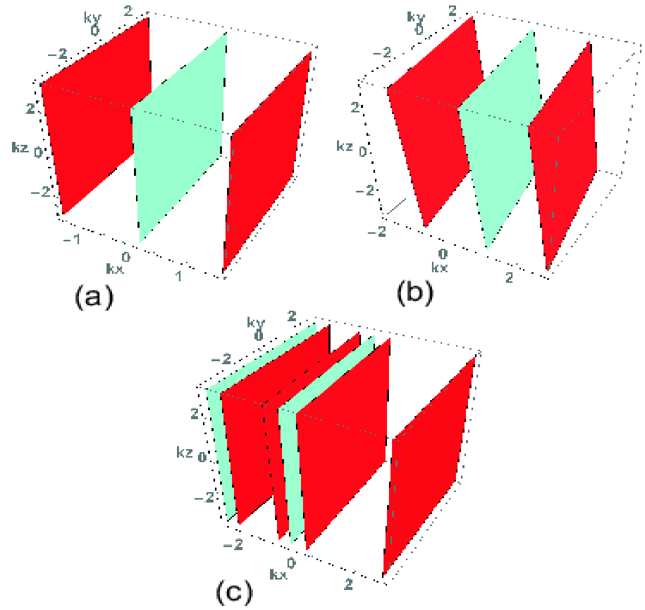

Figure 4: Plotting of the imaginary component of electric susceptibility is carried out for the kx, ky, and kz locations. Where distinct variables are (a) Δ_1= - 0.361γ, Δ_p= 2γ, $\gamma_{1,2}$=0.02γ, Ω_{2a} = 1γ, Ω_{20} = 6γ, $\phi_{21} = \frac{\pi}{3}$, $\phi_{22} = \frac{\pi}{2}$, $\phi_{23} = \frac{2\pi}{2}$, η_1 = - 0.01, $\eta_{2,3}$ = 0 (b) Δ_1= - 0.3γ, Δ_p= 9γ, γ_1=0.02γ, γ_2=0.09γ, Ω_{2a}=0.01γ, Ω_{20}=6γ, $\phi_{21,22,23}$ = π, η_1 = 0.1, $\eta_{2,3}$ = 0.01 (c) Δ_1= - 0.3γ, Δ_p= 0.9γ, γ_1=0.02γ, γ_2=0.09γ, Ω_{2a}=0.01γ, Ω_{20}=6γ, $\phi_{21,22,23}$ = π, η_1 = -1, $\eta_{2,3}$ = -0.01.

In Figure 5, for positions kx, ky, and kz, the plots are sketched for the imaginary component of electric susceptibility. Using the parameters, the localization of cylindrical-like atoms is investigated Δ_1= 0.9γ, Δ_p= 2γ, γ_1= 0.02γ, γ_2= 0.09, Ω_{2a}=1γ, Ω_{20}=6γ. In the first quadrant, a single cylindrical localization is seen using the phase $\phi_{21, 22, 23}$ = π, & the directions of applied fields η_1 =0.01, & $\eta_{2, 3}$ = -1, as seen in Fig 5.a. By changing the directions to η_1 = 1, η_2 = -0.01, & η_3 = -1. The second quadrant of the box is where one of the cylindrical localization shifts, as seen in Fig 5.b. varying the phase $\phi_{21, 23}$ = π, ϕ_{22}= π, & position of fields to η_1=-0.01, $\eta_{2, 3}$= -1. The cylindrical localization moves into the third quadrant, as seen in Fig 5.c. The cylindrical localization moves into the fourth quadrant of the box using the phase $\phi_{21, 22, 23}$ = π & the position of fields $\eta_{1, 3}$ = - 1, η_2 = -0.01 as seen in Fig 5.d.

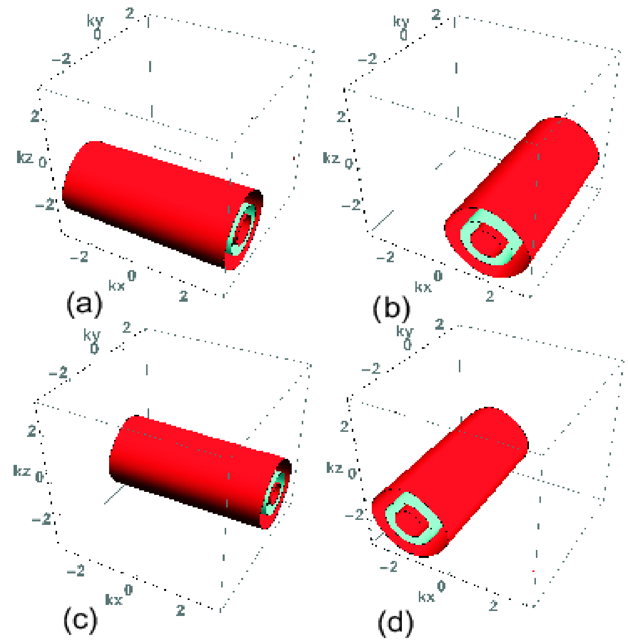

Figure 5: Plotting of the imaginary component of electric susceptibility is carried out for the kx, ky, and kz locations. Where distinct variables are Δ_1= 0.9γ, Δ_p= 2γ, γ_1= 0.02γ,γ_2= 0.09, Ω_{2a}=1γ, Ω_{20}=6γ.(a) $\phi_{21,22,23}$ = π, η_1 =0.01, and $\eta_{2,3}$ = -1 (b) $\phi_{21,22,23}$ = π, η_1 = 1, η_2 = -0.01, and η_3 = -1 (c) $\phi_{21,23}$ = π, ϕ_{22}= π, η_1=-0.01, $\eta_{2,3}$= -1 (d) $\phi_{21,22,23}$ = π, $\eta_{1,3}$ = - 1, η_2 = -0.01.

In Figure 6, for positions kx, ky and kz, the plots are sketched for the imaginary component of electric susceptibility. The localization of a single half-ellipsoidal-like atom is investigated using the parameters, Δ_1= 0.9γ, Δ_p = 2γ, γ_1= 0.02γ, γ_2= 0.09, Ω_{2a}=1γ, Ω_{20}= 6γ, $\phi_{21, 22, 23}$ = π. One ellipsoid localization is observe in the first quadrant Using the applied fields directions $\eta_{1, 3}$ = -1, η_2 = 0.09, as shown in Fig 6.a. By changing the directions to $\eta_{2, 3}$ = -1, and η_1 = 0.09, as seen in Fig. 6.b, one of the localizations shifts by applied field directions to η_1 = -1, η_2 = 0.09, and η_3 = 1, as shown in Fig. 6.c. the localization location varies to different places. The position uses the directions of fields to explore microscopy in various directions and locations η_1= -0.09, & $\eta_{2, 3}$ = 1, as shown in Fig 6.d.

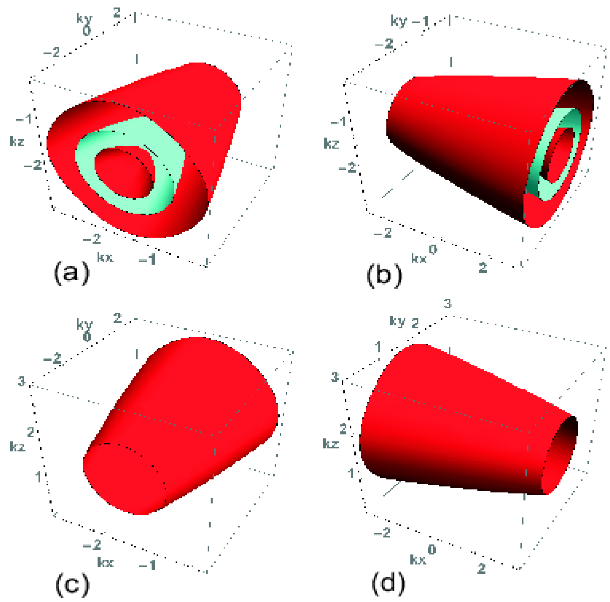

Figure 6: Plotting of the imaginary component of electric susceptibility is carried out for the kx, ky, and kz locations. Where distinct variables are $\Delta_1 = 0.9\gamma$, $\Delta_p = 2\gamma$, $\gamma_1 = 0.02\gamma$, $\gamma_2 = 0.09$, $\Omega_{2a} = 1\gamma$, $\Omega_{20} = 6\gamma$, $\phi_{21, 22, 23} = \pi$ (a) $\eta_{1, 3} = -1$, $\eta_2 = 0.09$ (b) $\eta_{2, 3} = -1$, $\eta_1 = 0.09$ (c) $\eta_1 = -1$, $\eta_2 = 0.09$, $\eta_3 = 1$ (d) $\eta_1 = -0.09$, $\eta_{2, 3} = 1$.

4 Conclusion

In summary, the absorption spectrum method was used to investigate three-dimensional atom localization. Single spherical at top and single spherical at bottom localizations are investigated. Cylindrical, ellipsoid and walls like with atom localization forms that vary in orientations, phases, detuning, and rabi frequencies of control fields have also been described. The location of atoms that have different distinct shapes is altered by changes in phases and directions. Innovative atom localization methods are beneficial for Bose-Einstein condensation, nanolithography, and laser cooling technologies.

Author Contributions

All authors have contributed equally: Methodology, Formal Analysis, and Writing – Original Draft Preparation, Writing – Review & Editing.

Acknowledgment

I thank anonymous referees for their suggestions to improve the paper.

Conflict of Interests

This work does not have any potential conflicts of interest.

Data Availability Statement

The associated data is available upon request from the corresponding author.

Grant/Funding Information

There are no funders to report for this submission.

Declaration Statement of Generative AI

The author declare they have not used Artificial Intelligence (AI) tools in the creation of this article

References

[1] He, Zhe, Yide Zhang, Xin Tong, Lei Li, and Lihong V. Wang. "Quantum microscopy of cells at the Heisenberg limit." *Nature Communications* 14, no. 1 (2023): 2441. https://doi.org/10.1038/s41467-023-38191-4

[2] Shah, Ismail, Manuel De la Sen, Saeed Ahmad, T. A. Alrebdi, and A. Abdel-Aty. "Atom localization by damping spectrum of surface plasmon polariton waves." *Alexandria Engineering Journal* 91 no. 1 (2024): 95-102. https://doi.org/10.1016/j.aej.2024.01.076

[3] Zhao, Shuncai, and Qixuan Wu. "Three-Level Λ-Type Atomic System Localized by the Parameters of the Two Orthogonal Standing-Wave Fields." *Journal of Applied Mathematics and Physics* 4, no. 08 (2016): 1546. https://doi.org/10.4236/jamp.2016.48164

[4] Collins, Graham P. "Experimenters produce new Bose-Einstein condesate (s) and Possible Puzzles for Theories" *Physics Today* 49, no. 3 (1996): 18-21. https://doi.org/10.1063/1.2807533

[5] Kapale, Kishor T., and Girish S. Agarwal. "Subnanoscale resolution for microscopy via coherent population trapping." *Optics letters* 35, no. 16 (2010): 2792-2794. https://doi.org/10.1364/ol.35.002792

[6] Mompart, J., Verònica Ahufinger, and Gerhard Birkl. "Coherent patterning of matter waves with subwavelength localization." *Physical Review A-Atomic, Molecular, and Optical Physics* 79, no. 5 (2009): 053638. https://doi.org/10.1103/physreva.79.053638

[7] Jin, Luling, Hui Sun, Yueping Niu, Shiqi Jin, and Shangqing Gong. "Two-dimension atom nano-lithograph via atom localization." *Journal of Modern Optics* 56, no. 6 (2009): 805-810. https://doi.org/10.1080/09500340802267134

[8] Li, Jiahua, Rong Yu, Min Liu, Chunling Ding, and Xiaoxue Yang. "Efficient two-dimensional atom localization via phase-sensitive absorption spectrum in a radio-frequency-driven four-level atomic system." *Physics Letters A* 375, no. 45 (2011): 3978-3985. https://doi.org/10.1016/j.physleta.2011.09.027

[9] Ding, Chunling, Jiahua Li, Rong Yu, Xiangying Hao, and Ying Wu. "High-precision atom localization via controllable spontaneous emission in a cycle-configuration atomic system." *Optics express* 20, no. 7 (2012): 7870-7885. https://doi.org/10.1364/oe.20.007870

[10] Rahmatullah, and Sajid Qamar. "Two-dimensional atom localization via probe-absorption spectrum." *Physical Review A-Atomic, Molecular, and Optical Physics* 88, no. 1 (2013): 013846. https://doi.org/10.1103/physreva.90.039901

[11] Salomon, C., J. Dalibard, A. Aspect, H. Metcalf, and C. Cohen-Tannoudji. "Channeling atoms in a laser standing wave." *Physical review letters* 59, no. 15 (1987): 1659. https://doi.org/10.1103/physrevlett.59.1659

[12] Thomas, J. E. "Uncertainty-limited position measurement of moving atoms using optical fields." *Optics letters* 14, no. 21 (1989): 1186-1188. https://doi.org/10.1364/ol.14.001186

[13] Thomas, J. E. "Quantum theory of atomic position measurement using optical fields." *Physical Review A* 42, no. 9 (1990): 5652. https://doi.org/10.1103/physreva.42.5652

[14] Stokes, K. D., C. Schnurr, J. R. Gardner, M. Marable, G. R. Welch, and J. E. Thomas. "Precision position measurement of moving atoms using optical fields." *Physical review letters* 67, no. 15 (1991): 1997. https://doi.org/10.1103/physrevlett.67.1997

[15] Gardner, J. R., M. L. Marable, G. R. Welch, and J. E. Thomas. "Suboptical wavelength position measurement of moving atoms using optical fields." *Physical review letters* 70, no. 22 (1993): 3404. https://doi.org/10.1103/physrevlett.70.3404

[16] Storey, Pippa, Matthew Collett, and Daniel Walls. "Measurement-induced diffraction and interference of atoms." *Physical review letters* 68, no. 4 (1992): 472. https://doi.org/10.1103/physrevlett.68.472

[17] Kunze, Stefan, Kai Dieckmann, and Gerhard Rempe. "Diffraction of atoms from a measurement induced grating." *Physical review letters* 78, no. 11 (1997): 2038. https://doi.org/10.1103/physrevlett.78.2038

[18] Quadt, Ralf, Matthew Collett, and Dan F. Walls. "Measurement of atomic motion in a standing light field by homodyne detection." *Physical review letters* 74, no. 3 (1995): 351. https://doi.org/10.1103/physrevlett.74.351

[19] Le Kien, Fam, G. Rempe, Wolfgang P. Schleich, and M. Suhail Zubairy. "Atom localization via Ramsey interferometry: a coherent cavity field provides a better resolution." *Physical Review A* 56, no. 4 (1997): 2972. https://doi.org/10.1103/physreva.56.2972

[20] Marte, M. A. M., and P. Zoller. "Quantum nondemolition measurement of transverse atomic position in Kapitza-Dirac atomic beam scattering." *Applied Physics B* 54 (1992): 477-485. https://doi.org/10.1007/bf00325394

[21] Kunze, Stefan, Kai Dieckmann, and Gerhard Rempe. "Diffraction of atoms from a measurement induced grating." *Physical review letters* 78, no. 11 (1997): 2038. https://doi.org/10.1103/physrevlett.78.2038

[22] Thomas, J. E., and L. J. Wang. "Precision position measurement of moving atoms." *Physics Reports* 262, no. 6 (1995): 311-366. https://doi.org/10.1016/0370-1573(95)00050-q

[23] Herkommer, Alois M., Wolfgang P. Schleich, and M. Suhail Zubairy. "Autler-Townes microscopy on a single atom." *Journal of Modern Optics* 44, no. 11-12 (1997): 2507-2513. https://doi.org/10.1080/09500349708231897

[24] Holland, M., S. Marksteiner, P. Marte, and P. Zoller. "Measurement induced localization from spontaneous decay." *Physical review letters* 76, no. 20 (1996): 3683. https://doi.org/10.1103/physrevlett.76.3683

[25] Ghafoor, Fazal, Sajid Qamar, and M. Suhail Zubairy. "Atom localization via phase and amplitude control of the driving field." *Physical Review A* 65, no. 4 (2002): 043819. https://doi.org/10.1103/physreva.65.043819

[26] Paspalakis, E., and P. L. Knight. "Localizing an atom via quantum interference." *Physical Review A* 63, no. 6 (2001): 065802. https://doi.org/10.1103/physreva.63.065802

[27] Agarwal, Girish S., and Kishore T. Kapale. "Subwavelength atom localization via coherent population trapping." *Journal of Physics B: Atomic, Molecular and Optical Physics* 39, no. 17 (2006): 3437. https://doi.org/10.1088/0953-4075/39/17/002

[28] Thomas, J. E., and L. J. Wang. "Precision position measurement of moving atoms." *Physics Reports* 262, no. 6 (1995): 311-366. https://doi.org/10.1016/0370-1573(95)00050-q

[29] Herkommer, Alois M., Wolfgang P. Schleich and M. Suhail Zubairy. "Autler-Townes microscopy on a single atom." *Journal of Modern Optics* 44, no. 11-12 (1997): 2507-2513. https://doi.org/10.1080/09500349708231897

[30] Macovei, Mihai, Jörg Evers, Christoph H. Keitel, and M. Suhail Zubairy. "Localization of atomic ensembles via superfluorescence." *Physical Review A-Atomic, Molecular, and Optical Physics* 75, no. 3 (2007): 033801. https://doi.org/10.1103/physreva.75.033801

[31] Sahrai, M. "Atom localization via absorption spectrum." *Laser physics* 17, no. 1 (2007): 98-102. https://doi.org/10.1134/s1054660x07020089

[32] Qamar, Sajid, Jörg Evers, and M. Suhail Zubairy. "Atom microscopy via two-photon spontaneous emission spectroscopy." *Physical Review A-Atomic, Molecular, and Optical Physics* 79, no. 4 (2009):

043814. https://doi.org/10.1103/physreva.79.043814

Publisher's Note: All claims expressed in this article are solely those of the authors and do not necessarily represent those of their affiliated organizations or the publisher, the editors and the reviewers. Any product that may be evaluated in this article, or claim made by its manufacturer, is not guaranteed or endorsed by the publisher.